Journal of Fluorescence, Vol. 14, No. 1, January 2004 (©2004)

Photoluminescence Properties of Conjugated Phenylacetylene Monodendrons in Thin Films

Joseph S. Melinger,[1,3] Benjamin L. Davis,[1] Dale McMorrow,[1] Yongchun Pan,[2] and Zhonghua Peng[2]

Received September 7, 2003; accepted October 22, 2003

We report the absorption, photoluminescence (PL), and time-dependent PL of thin films of conjugated phenylacetylene monodendrons at both room temperature and at cryogenic temperature. We find that the PL properties of the monodendron thin films are significantly different from their fluorescence in dilute solution due to the presence of interactions between monodendrons in the thin film. These interactions lead to aggregate species in the thin films, which result in broader PL spectra and lower PL quantum yields than for monodendrons in dilute solution. Evidence for excimer-like aggregates in the monodendron thin films is found from time-resolved PL spectra.

KEY WORDS: Dendrimers; photoluminescence; thin films; aggregates.

INTRODUCTION

Conjugated dendrimers are exciting new materials with potential for a variety of photonics-based applications including light harvesting [1–3], fluorescent sensors [4], light emitting diodes [5], and devices based on nonlinear optical interactions [6,7]. This potential results from the unique dendritic structure. For conjugated dendrimers, the highly branched structure can lead to a high density of chromophore sites, which, in turn, leads to large molar extinction coefficients [1a,2,3]. Further, the branches converge to a single site at the core, which provides an architecture for rapid and unidirectional energy transfer to the core [1,8,9]. Recently, Peng *et al.* reported a new class of conjugated phenylacetylene (PA) dendrimers based on an unsymmetrical branching structure [2]. Scheme 1 illustrates the unsymmetrical branching structure for a series of PA monodendrons that are considered in this paper. Branching occurs at both the *ortho* and *para* positions of a benzene ring, which leads to non-equivalent branches. In contrast, symmetrical branching occurs entirely at the *meta* position and leads to equivalent branches (all branches are the same) [1a]. In a previous study, we showed that, in dilute solutions, the unsymmetrical monodendrons of Scheme 1 have broad electronic absorption widths, high molar extinction coefficients, good fluorescence quantum yields (65–80%), and single exponential fluorescence lifetimes [3]. Further, when an energy accepting perylene trap is placed at the core, the PA monodendrons exhibit high energy transfer quantum yields, which are in the 90% range [3].

Our previous studies of PA monodendrons have been restricted to the case of dilute solutions [2,3]. However, many applications such as light emitting diodes and photovoltaics require that thin films of the active material be fabricated. Thus, to better understand the potential of PA dendrimer thin films for applications, it is important to better understand their excited state properties [10,11]. Another motivation for investigating the photophysics of dendrimer thin films is the potential for the large backbone to shield the core region from intermolecular interactions that form photophysical aggregates. Recent studies of dendrimer thin films have provided evidence that

[1] Naval Research Laboratory, Electronics Science and Technology Division, Washington, District of Columbia 20375.
[2] Department of Chemistry, University of Missouri-Kansas City, Kansas City, Missouri 64110.
[3] To whom correspondence should be addressed. E-mail: melinger@ccf.nrl.navy.mil

1053-0509/04/0100-0105/0 © 2004 Plenum Publishing Corporation

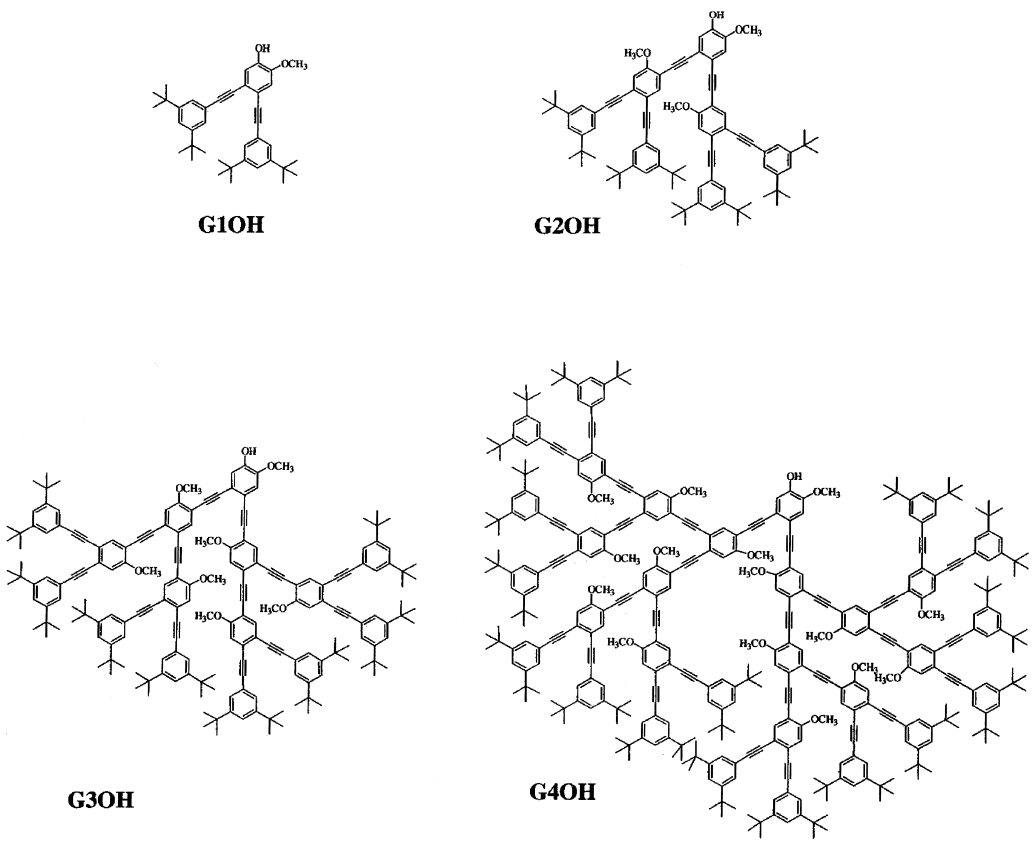

Scheme. 1. Structures of unsymmetrical phenylacetylene dendrimers.

the dendritic backbone does provide a measure of core shielding [10,11]. In this paper we explore the photophysical properties of unsymmetrical PA monodendrons in thin films and compare them to their corresponding properties in dilute solutions. The PA monodendrons are characterized with steady-state absorption and photoluminescence (PL) spectroscopy, emission quantum yields, and time-resolved PL spectroscopy. We find that the excited state properties of the monodendron thin films are significantly affected by aggregate species, leading to properties different from those observed in solutions. The photophysical properties of PA monodendron thin films appear to be qualitatively similar to those often found in linear conjugated polymer thin films.

EXPERIMENTAL

The synthetic procedures for all monodendrons studied here have been reported previously [2a]. Thin films were made by spin casting from a concentrated dichloromethane (DCM) solution (∼5 mg/mL) onto a fused silica substrate at speeds ranging from 750–1000 rpm. This resulted in films with peak optical densities of about 1.0. The films were stored in the dark under a nitrogen atmosphere.

Absorption spectra were measured with a Perkin-Elmer Lambda 9 spectrometer. Steady state emission spectra were measured with a Spex 1680 monochromator. For solution measurements the sample concentrations were adjusted to give an optical density of less than 0.1 in a 1 cm path cell. Monodendron concentrations were between 10^{-7} and 10^{-6} M. Fluorescence quantum yields were measured using a quinine sulfate solution in 1N H_2SO_4 as a standard (quantum yield = 0.55) [12]. The PL quantum yields of the thin films were measured using an integrating sphere [13] and the 325 nm line of a HeCd laser. The error in the PL quantum yield measurements for thin films is estimated to be $\pm 15\%$. For spectral measurements at low temperature, the films were placed in a cryostat cooled by liquid helium.

Time-resolved PL measurements were performed using the technique of time-correlated single photon counting (TCSPC) [14]. The excitation source was a synchronously-pumped and cavity-dumped dye laser (1 MHz), which was frequency-doubled to the 300 nm

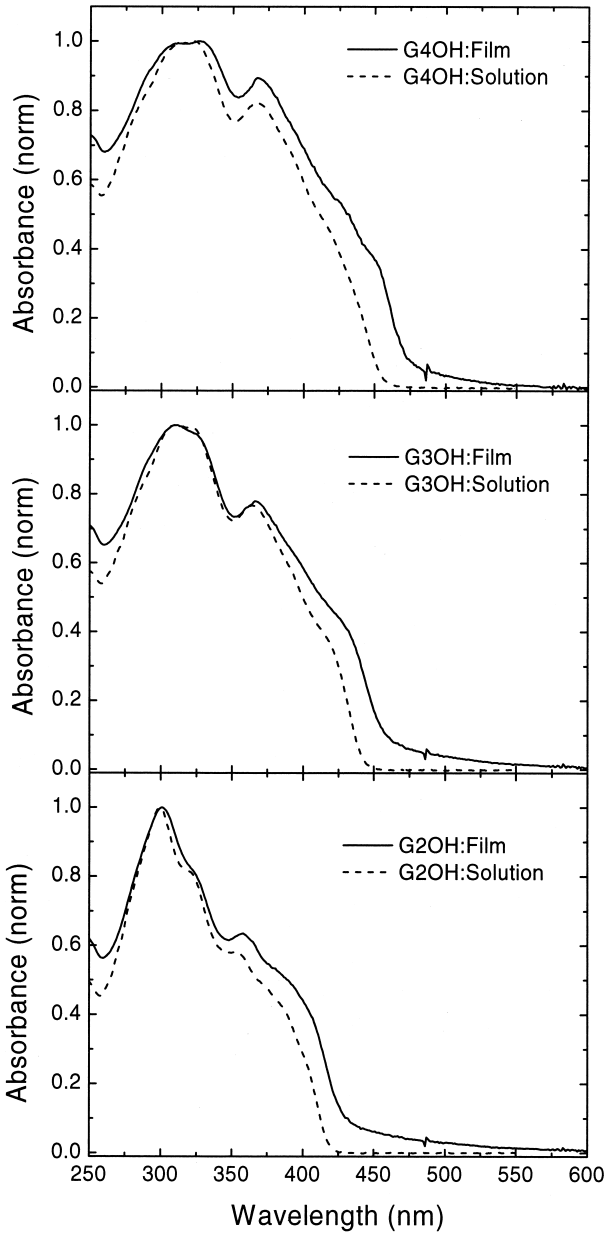

Fig. 1. Absorption spectra of GnOH in dichloromethane (dotted line) and in thin films (solid line) at 298 K. The spectra are normalized at 300 nm.

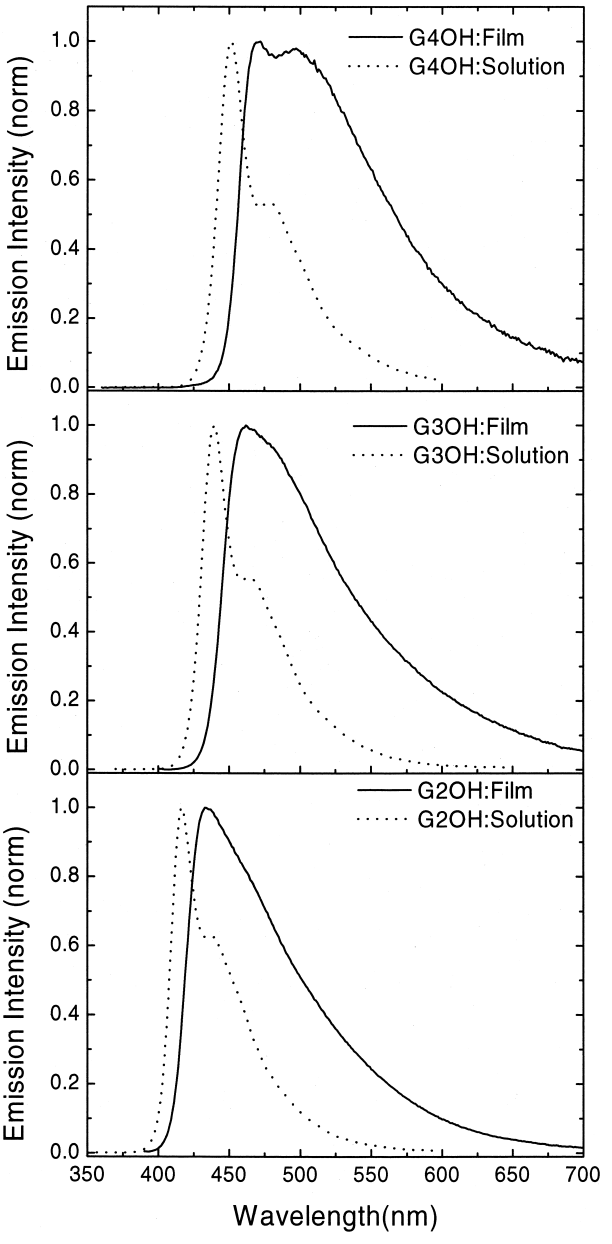

Fig. 2. Normalized photoluminescence spectra of GnOH in solution (dotted line) and in thin films (solid line) at 298 K.

range. The emission was filtered with a monochromator and detected with a microchannel plate photomultiplier. The instrument response, taken to be the full width at half maximum when detecting the scattered light from a thin ground glass surface, was determined to be 50–55 ps. All TCSPC measurements were performed at the magic angle [13]. The decays were analyzed using the reconvolution technique and fitting the data to a sum of exponentials with a Levenson-Marquardt algorithm.

RESULTS AND DISCUSSION

The unsymmetrical PA monodendrons shown in Chart 1 are labeled GnOH and have a phenol group at the core. The generations (n) 2–4 are studied in this paper. Figure 1 compares GnOH absorption spectra in DCM solution and in thin films. For GnOH in solution the absorption edge shifts to the red as the generation increases. The red shift arises due to the presence of longer conjugated

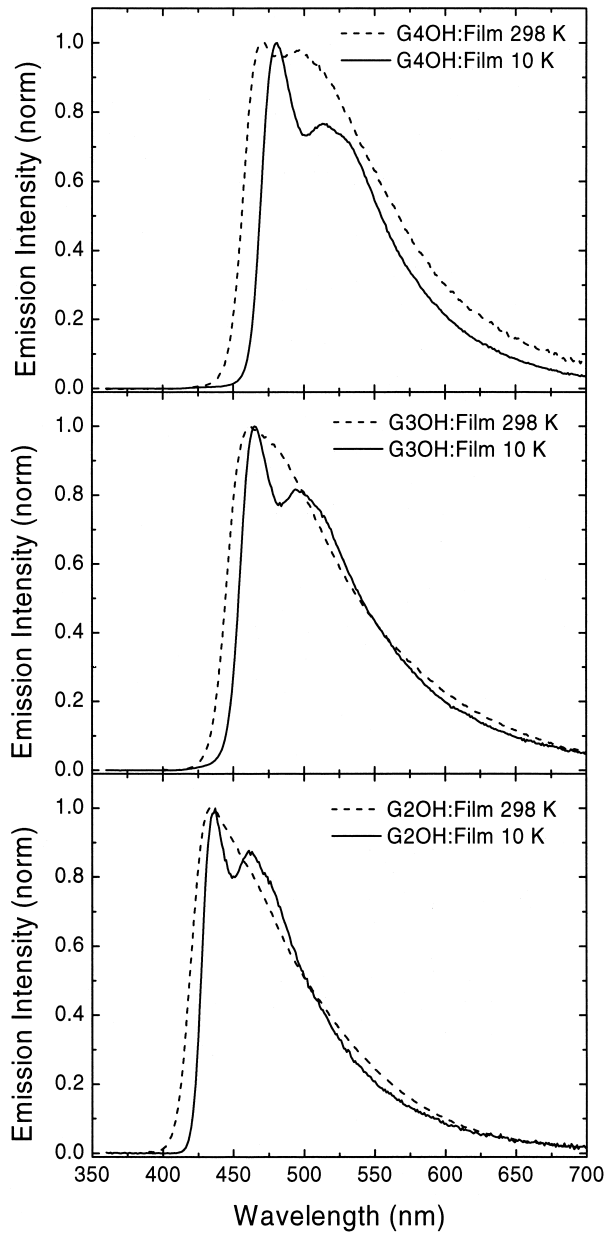

Fig. 3. Normalized photoluminescence spectra of GnOH thin films at 298 K (dotted line) and at 10 K (solid line).

PA chains in the higher generations [2,3]. The broad absorption width of the higher generations is, in part, due to a superposition of absorption bands associated with different length PA chains. The absorption spectra of the GnOH thin films are found to be quite similar in shape to those in solution. The main spectral features observed in solution are also observed in the thin films. There is, approximately, a 20 nm red shift of the absorption edge for each GnOH thin film, which is attributed, in part, to the increased polarizability of the surrounding medium in the thin film [15].

In contrast to the absorption spectra, Fig. 2 shows that there are significant differences in the emission properties between monodendrons in solution and in thin films. The excitation wavelength in all cases is 350 nm. The fluorescence spectra of GnOH in solution are relatively narrow, and show structure due to the vibrational modes of the PA backbone [3]. The PL spectra of the GnOH thin films are significantly broader and display a red shift with respect to the solution spectra. Qualitatively, the spectra appear to contain at least two components: a relatively sharp component on the blue side of the spectrum, and a relatively broad feature on the red side. In an attempt to better resolve these features, PL spectra of the thin films were also measured at low temperature (10 K), and are shown in Fig. 3. The spectra at 10 K are significantly sharper than at 298 K and show clearer evidence for at least two components. In each spectrum at 10 K a relatively sharp peak is clearly resolved on the blue side of the spectrum, though the spectral widths (half-width at half maximum, or HWHM) of these peaks (∼12–13 nm HWHM) are broader than observed for the corresponding 0–0 emission lines (∼9 nm HWHM) in the solution spectra at 298 K (Fig. 2). This increased line width indicates the presence of inhomogeneous broadening in the thin film. While homogeneous sources of line broadening are attenuated at cryogenic temperatures, there clearly remains residual broadening, which is likely due to a distribution of local environments that result from the way the monodendrons pack in the thin film.

Table I summarizes the emission characteristics of the GnOH in solution and in thin films. The emission quantum yields of the thin films are substantially lower than in the solutions. The G2OH thin film gives the highest PL quantum yield of 27%; whereas for G4OH the quantum yield falls to 13% (the G3OH PL quantum yield was not measured). The lower PL quantum yield of the films

Table I. Emission Properties

Compound	Environment	λ (nm)[a]	ϕ[b]	τ[c]
G2OH	DCM, 298 K	417	0.81	2.0
G2OH	Thin Film, 298 K	433	0.27	—
G3OH	DCM, 298 K	440	0.70	1.9
G3OH	Thin Film, 298 K	462	—	—
G4OH	DCM, 298 K	452	0.65	1.7 (95%); 2.7 (5%)
G4OH	Thin Film, 298 K	472	0.13	—
G4OH	Thin Film, 10 K	481	—	—

[a] Wavelength at the emission maximum.
[b] Fluorescence quantum yield (solution) measured against quinine sulfate standard, or photoluminescence quantum yield (thin film) measured using an integrating sphere.
[c] Excited state lifetime.

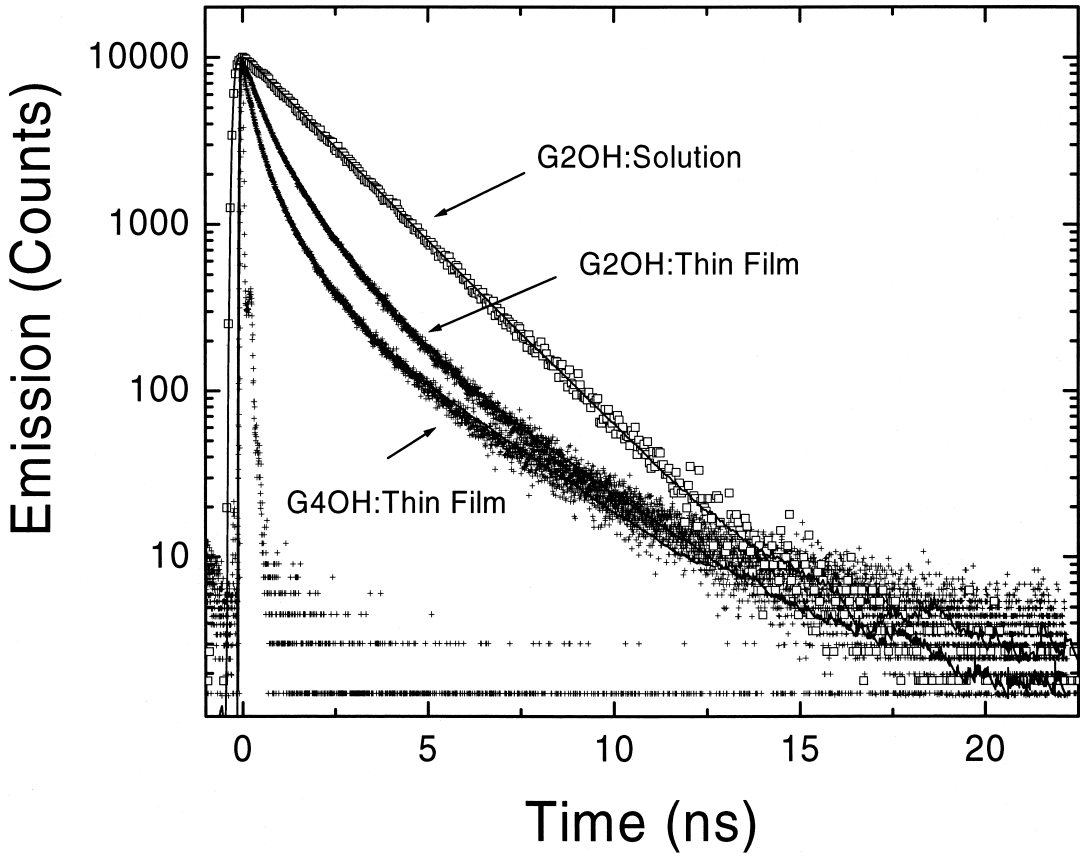

Fig. 4. Time-resolved photoluminescence decays at 298 K: G2OH in dichloromethane, G2OH thin film, and G4OH thin film, as indicated in graph. The curve at early times is the instrument response. The solid lines are fits to the data based on a sum of exponentials.

indicates the presence of significant non-radiative relaxation pathways. These may include energy migration to quenching sites within the film, and energy transfer to aggregate states that are only weakly emissive. Even so, the PL quantum yields of G2OH and G4OH thin films fall in the range typically found in linear conjugated polymers [13].

A comparison to the PL properties often observed in linear conjugated polymers is useful. PL spectra of conjugated polymer thin films often show a relatively sharp component that is reminiscent of their spectra in solution, as well as a broad red-shifted component due to aggregate species [15–17]. The relative fraction of solution-like and aggregate species depends, in part, on the 3-D conformation of the conjugated polymer [15]. Even though the three dimensional structure of the conjugated PA monodendrons is different than that of linear conjugated polymers, the GnOH thin films may still be expected to show similar PL properties. For the GnOH series, molecular modeling based on molecular mechanics minimization shows that the three dimensional shape becomes more globular-like as the generation increases beyond $n = 2$. However the core region that contains the emitting PA chain is exposed. At first, it may be anticipated that the globular shape of the larger GnOH may hinder the formation of aggregates compared to the case of rigid linear conjugated polymers, where the rods can more tightly pack leading to stronger intermolecular interactions. Apparently, however, there are regions of the GnOH thin films where the monodendrons pack tightly and the core region of monodendrons can come sufficiently close to form photophysical aggregates, which gives rise to the broad features on the red side of the GnOH PL spectra.

A recent study of conjugated dendrimer thin films based on stilbene units has shown that PL spectra of the core states become sharper as the generation size increases [11]. The PL quantum yields correspondingly increase with increasing generation [11]. This effect is thought to be due to the larger dendrimer backbone of higher generations becoming more effective in attenuating

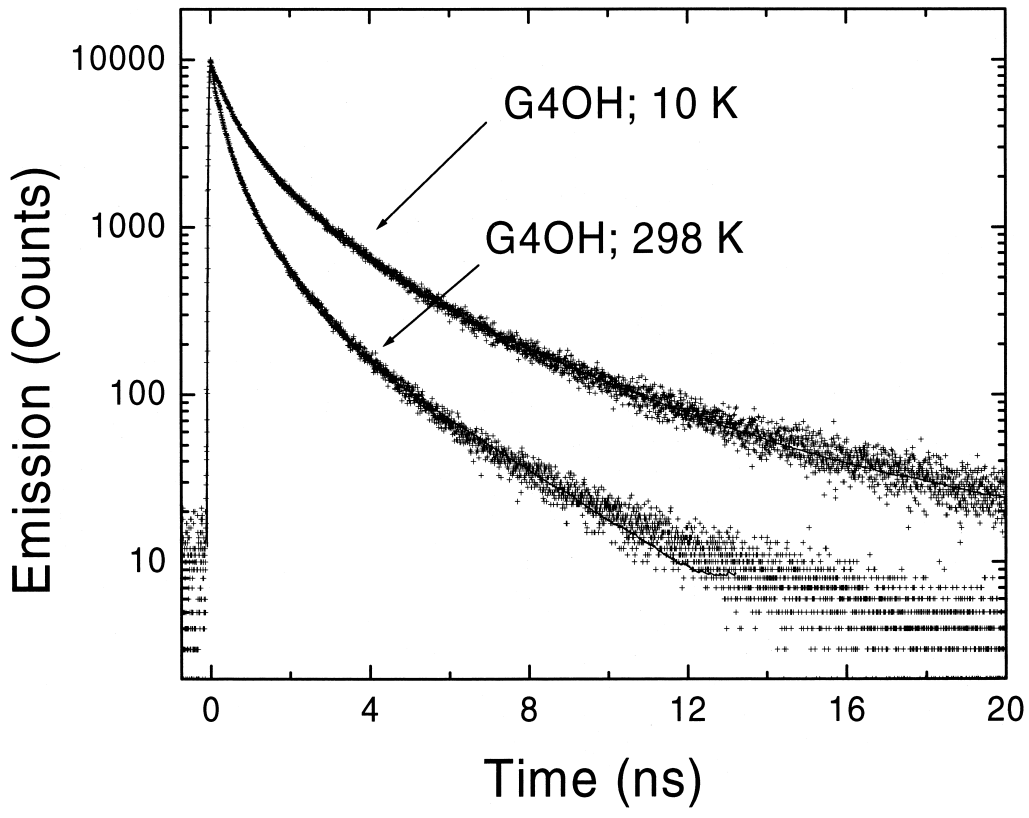

Fig. 5. Comparison of G4OH thin film time-resolved photoluminescence at 298 K and at 10 K, as indicated in the graph. The solid lines are fits to the data based on a sum of exponentials.

intermolecular interactions between the cores of adjacent dendrimers [11]. For the PA monodendron films investigated here the trend is the opposite: the spectra broaden and the PL quantum yields decrease with increasing generation size. One explanation is that the GnOH thin films contain only monodendrons instead of a full dendrimer structure, which contains three Gn monodendrons attached to a focal benzene group [2c]. In GnOH monodendron thin films, tight packing apparently leads to strong intermolecular interactions between the exposed core states (longest conjugated chains) of adjacent monodendrons. It's possible that for the full PA dendrimer structure there may be steric effects that attenuate such interations between core states. Such a study remains to be done.

Time-resolved PL measurements provide information regarding the excited state dynamics in the GnOH thin films. As a representative example, Fig. 4 compares the fluorescence decay of G2OH in solution with the PL decays of both G2OH and G4OH thin films at 298 K. In each case the measurement integrates over nearly the entire emission bandwidth. In previous work we found that the fluorescence decays for GnOH ($n = 1$–3) in DCM solution are adequately described by single exponential decay times of about 2.0 ns (for G4OH the dominant component accounts for 95% of the decay) [3]. In contrast, the thin film PL dynamics are highly non-exponential. Fits based on a sum of three exponential terms gave χ^2 values less than 1.6, and the results of the fittings along with the weighted average of the time constants (τ_{avg}) are collected in Table II. We note that fits based on a sum of exponentially decaying components may not accurately describe the complex excited state dynamics of the thin films [18], nevertheless they are useful in providing a measure of the PL decay rate. A major fraction of the thin film PL decay occurs at a rate significantly faster than the solution decay time of about 2.0 ns. The fast relaxation may reflect a distribution of different emitting states, excitation hopping

Table II. Photoluminescence Lifetimes

	τ_1 (ns)	τ_2 (ns)	τ_3 (ns)	τ_{avg} (ns)
G2OH, 298 K	0.26 (46%)	0.98 (47%)	2.63 (7%)	0.77
G4OH, 298 K	0.14 (64%)	0.71 (32%)	2.8 (4%)	0.43
G4OH, 10 K	0.28 (53%)	1.3 (38%)	4.2 (9%)	1.0

Note. Relative amplitudes in percent are given in parenthesis.

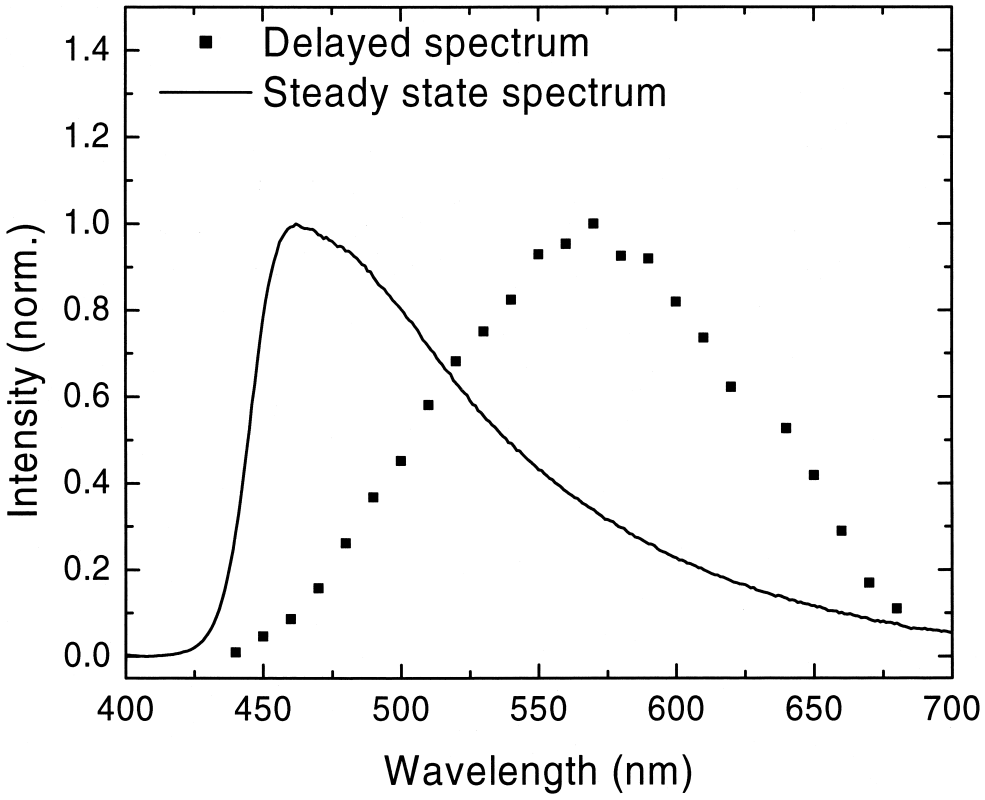

Fig. 6. Delayed photoluminescence spectra (points) for the G3OH thin film at 298 K reconstructed from TCPSC decay curves (as described in the text). The steady state spectrum for the G3OH thin film at 298 K is shown as the solid line.

between monodendrons (similar to the hopping of excitons in linear conjugated polymer thin films) [18], as well as migration to quenching sites. There is also a weak emission seen in the tail part of the relaxation that decays on a somewhat longer timescale than in solution. This longer time component likely reflects the relaxation from weakly emissive aggregate states. Figure 4 also shows that the decay rate of the G4OH thin film is significantly faster than the decay rate of the G2OH thin film, which is consistent with the lower PL quantum yield measured for the G4OH thin film. One explanation is that aggregates make up a greater fraction of the species in the G4OH thin film. This explanation is supported by the broader emission spectrum observed for the G4OH thin film (at 298 K) compared to the G2OH thin film (see Fig. 2).

Figure 5 compares the G4OH thin film PL decays at 298 K and 10 K, and shows that the decay rate is significantly slower at 10 K. The results of the curve fitting (Table II) show that τ_{avg} increases from 0.43 ns at 298 K, to 1.0 ns at 10 K. If the early time portion of the decay is associated, in part, with migration of excitations to quenching sites, then it is reasonable to conclude that such migration in the GnOH films is an activated process. From Table II, we note that at 10 K the relative fraction of the slow component has increased by more than a factor of 2 with respect to its fraction at 298 K, which implies that emission from the longer-lived aggregate states becomes more efficient at low temperature.

Additional insight regarding the excited state species in the thin film can be obtained from time-resolved PL spectra. Here we focus on the "long-time" component in the PL decay in the time interval from 2.0 to 20 ns. The delayed PL spectrum is reconstructed from individual TCSPC decay curves measured in 10 nm steps over the width of the emission spectrum. Each TCSPC curve is collected with a spectral resolution of about 10 nm and integrated from 2.0 to 20 ns to represent a single point in the delayed spectrum. Figure 6 shows the delayed PL spectrum for the G3OH thin film at 298 K. For comparison, the steady state PL spectrum is also shown. Since the two spectra were recorded using different spectrometers the comparison in Fig. 6 is only qualitative. Even so, it is clear that the delayed spectrum is strongly red shifted from the steady state spectrum by around 100 nm, and consists of a spectrally

broad (∼150 nm full width at half maximum) and featureless emission profile. These characteristics of the delayed PL spectrum are consistent with an excimer emission [17]. Delayed PL spectra for G2OH and G4OH were found to have characteristics similar to those observed for G3OH.

SUMMARY

In this paper we have presented an initial exploration of the photophysics of unsymmetrical phenylacetylene monodendrons in thin films, and we have compared their characteristics to the case when they are in a dilute solution environment. From the thin film PL spectra, we conclude that inter-dendron interactions are significant for all generations ($n = 2$–4) investigated here. This conclusion is supported by broader and red shifted PL spectra and lower PL quantum yields (by a factor of 3–5) for the GnOH thin films with respect to the GnOH in dilute solution. The time-dependent PL of each of the GnOH films is highly non-exponential, which indicates that the excited state dynamics are complex. The presence of weakly emissive excimer-like aggregates was confirmed by the delayed emission, which was found to be broad, featureless, and strongly red-shifted from the main part of the emission.

REFERENCES

1. (a) C. Devadoss, P. Bharathi, and J. S. Moore (1996). Energy transfer in dendritic macromolecules: Molecular size effects and the role of an energy gradient. *J. Am. Chem. Soc.* **118**, 9635–9644; (b) M. R. Shortreed, S. F. Swallen, Z. Y. Shi, W. Tan, Z. Xu, C. Devadoss, J. S. Moore, and R. Kopelman; (1997). Directed energy transfer funnels in dendrimeric antenna supermolecules. *J. Phys Chem. B* **101**, 6318–6322.
2. (a) Z. Peng, Y. Pan, B. Yu, and J. Zhang (2000). Synthesis and optical properties of novel unsymmetrical conjugated dendrimers. *J. Am. Chem. Soc.* **122**, 6619–6623; (b) Y. Pan, M. Lu, Z. Peng, and J. S. Melinger (2003). Synthesis and optical properties of unsymmetrical conjugated dendrimers focally anchored with perylenes in different geometries. *J. Org. Chem.* **68**, 6952–6958; (c) Y. Pan, Z. Peng, and J. S. Melinger (2003). Synthesis and optical properties of conjugated dendrimers with unsymmetrical branching. *Tetrahedron* **59**, 5495–5506.
3. J. S. Melinger, Y. Pan, V. D. Kleiman, Z. Peng, B. L. Davis, D. McMorrow, and M. Lu (2002). Optical and photophysical properties of light-harvesting phenylacetylene monodendrons based on unsymmetrical branching. *J. Am. Chem. Soc.* **124**, 12002–12012.
4. (a) V. J. Pugh, Q.-S. Hu, and L. Pu (2000). The first dendrimer-based enantioselective fluorescent sensor for the recognition of chiral amino alcohols. *Angew. Chem. Int. Ed.* **39**, 3638–3641; (b) V. J. Pugh, Q.-S. Hu, X. Zuo, F. D. Lewis, and L. Pu (2001). Optically active BINOL coreb-based phenyleneethynylene dendrimers for the enantioselective fluorescent recognition of amino alcohols. *J. Org. Chem.* **66**, 6136–6140.
5. (a) P. W. Wang, Y. Liu, C. Devadoss, P. Bharathi, and J. S. Moore (1996). *Adv. Mat.* **8** 237; (b) M. Halim, J. N. Pillow, I. D. W. Samuel, and P. L. Burn (1999). Conjugated dendrimers for light-emitting diodes: Effect of generation. *Adv. Mat.* **11**, 371–374.
6. M. Lu, Y. Pan, and Z. Peng (2002). Soluble dipolar dendrimers with peripheral sulfone groups. *Tetrahedron Lett.* **43/44**, 7903.
7. (a) D. W. Brousmiche, J. M. Serin, J. M. J. Frechet, G. S. He, T.-C. Lin, S. J. Chung, and P. N. Prasad (2003). Fluorescence resonance energy transfer in a novel two-photon absorbing system. *J. Am. Chem. Soc.* **125**, 1448–1449; (b) A. Adronov, J. M. J. Frechet, G. S. He, K.-S. Kim, S.-J. Chung, J. Swiatkiewicz, and P. N. Prasad (2000). Novel two-photon absorbing dendritic structures. *Chem. Mater* **12**, 2838.
8. R. Kopelman, M. Shortreed, Z.-Y. Shi, W. Tan, Z. Xu, J. S. Moore, A. Bar-Haim, and J. Klafter (1997). Spectroscopic evidence for excitonic localization in fractal antenna supermolecules. *Phys. Rev. Lett.* **78**, 1239–1243.
9. V. D. Kleiman, J. S. Melinger, and D. McMorrow (2001). Ultrafast dynamics of electronic excitations in a light-harvesting phenylacetylene dendrimer. *J. Phys. Chem. B* **105**, 5595–5598.
10. L. F. Lee, A. Adronov, R. D. Schaller, J. M. J. Frechet, and R. J. Saykally (2003). Intermolecular coupling in nanometric domains of light-harvesting dendrimer films studied by photoluminescence near-field scanning optical microscopy (PL NSOM). *J. Am. Chem. Soc.* **125**, 536–540.
11. L.-O. Palsson, R. Beavington, M. J. Frampton, J. M. Lupton, S. W. Magennis, J. P. J. Markham, J. N. G. Pillow, P. L. Burn, and I. D. W. Samuel (2002). Synthesis and excited state spectrscopy of tris(distyrylbenzyl)amine-cored electroluminescent dendrimers. *Macromolecules* **35**, 7891–7901.
12. J. N. Demas and G. A. Crosby (1971). The measurement of photoluminescence quantum yields. A review. *J. Phys. Chem.* **75**, 991–1024.
13. N. C. Greenham, I. D. W. Samuel, G. R. Hayes, R. T. Phillips, Y. A. R. R. Kessener, S. C. Moratti, A. B. Holmes, and R. H. Friend (1995). Measurement of absolute photoluminescence quantum efficiencies in conjugated polymers. *Chem. Phys. Lett.* **241**, 89–96.
14. D. V. O'Conner and D. Phillips (1984). *Time Correlated Single Photon Counting*, Academic Press, New York.
15. T.-Q. Nguyen, I. B. Martini, J. Liu, and B. Schwartz (2000). Controlling interchain interactions in conjugated polymers: The effects of chain morphology on exciton–exciton annihilation and aggregation in MEH-PPV films. *J. Phys. Chem. B* **104**, 237–255.
16. T.-Q. Nguyen, B. J. Schwartz, R. D. Schaller, J. C. Johnson, L. F. Lee, L. H. Haber, and R. D. Saykally (2001). Near-field scanning optical microscopy (NSOM) studies of the relationship between interchain interactions, morphology, photodamage, and energy transport in conjugated polymer films. *J. Phys Chem. B* **105**, 5153–5160.
17. R. Jakubiak, C. J. Collison, W. C. Wan, and L. J. Rothberg (1999). Aggregation quenching of luminescence in electroluminescent conjugated polymers. *J. Phys. Chem. A* **103**, 2394–2398.
18. K. Brunner, A. Tortschanoff, Ch. Warmuth, H. Bassler, and H. F. Kaufmann (2000). Site torsional motion and dispersive excitation hopping in π-conjugated polymers. *J. Phys. Chem. B* **104**, 3781–3790.